The Oceanic Variability Spectrum and Transport Trends

Carl Wunsch*

Department of Earth, Atmospheric and Planetary Sciences
Massachusetts Institute of Technology, Cambridge MA 02139 USA

[Original manuscript received 17 October 2008; accepted 16 June 2009]

ABSTRACT *Oceanic meridional transports evaluated over the width of the Pacific Ocean from altimetric observations become incoherent surprisingly rapidly with meridional separation. Even with 15 years of data, surface slopes show no significant coherence beyond 5° of latitude separation at any frequency. An analysis of the frequency/zonal-wavenumber spectral density shows a broad continuum of motions at all time and space scales, with significant excess energy along a 'non-dispersive' line extending from the barotropic to the first baroclinic mode Rossby waves. It is speculated that much of that excess energy lies with coupled barotropic and first mode Rossby waves. The statistical significance of apparent oceanic transport trends depends upon the existence of a reliable frequency/wavenumber spectrum for which only a few observational elements currently exist.*

RÉSUMÉ *[Traduit par la rédaction] Les transports océaniques méridionaux évalués sur toute la largeur de l'océan Pacifique à partir d'observations altimétriques deviennent incohérents de façon étonnamment rapide avec la séparation méridienne. Même avec 15 ans de données, les pentes de la surface n'affichent pas de cohérence significative au-delà de 5° de séparation latitudinale, quelle que soit la fréquence considérée. Une analyse de la densité spectrale de fréquence/de nombre d'ondes zonal montre un assez large continuum des mouvements à toutes les échelles temporelles et spatiales, avec une quantité appréciable d'énergie en excès le long d'une ligne « non dispersive » s'étendant du mode barotrope jusqu'au premier mode barocline des ondes de Rossby. Nous posons l'hypothèse qu'une grande partie de cet excédent d'énergie se trouve dans les ondes de Rossby barotrope et du premier mode couplées. La signification statistique des tendances apparentes du transport océanique dépend de l'existence d'un spectre de fréquence/de nombre d'ondes fiable et pour lequel seuls quelques éléments d'observation existent actuellement.*

1 Introduction

A quantitative description of oceanic variability is useful for a number of reasons including the detection of climate trends, the testing of oceanic general circulation models (GCMs), and the identification and understanding of basic physical mechanisms in the ocean circulation. In particular, detection of supposed trends in the ocean circulation is now the subject of impressive expenditures (Schiermeier, 2004), and has captured the interest of a large community concerned about climate change (e.g., IPCC, 2007), including efforts directed at providing an early warning of abrupt jumps. But the ocean is a very noisy place with variability on all time and space scales and with a very long intrinsic memory (e.g., Peacock and Maltrud, 2006; Wunsch and Heimbach, 2008). Because of the long memory, most oceanographic time series display some form of apparent trend and the main issue is assigning a confidence interval to the result to distinguish it from the random-walk behaviour always present in long time-scale systems (e.g., Percival et al., 2001). Determination of the significance of true trends involves a deep understanding of the nature of oceanic variability generally. (Here, a 'true trend' is defined as one that would persist for several multiples of the data duration.) The goal of understanding the apparent fluctuations in meridional volume transports as determined from sea level variations is used to motivate a discussion of the nature of altimetric data sets. Trends in sea level variations are of intense interest in their own right but are not directly pursued here (see Wunsch et al. (2007) for discussion and references).

2 Altimetric velocities and transports

The longest observed time series available with near-global coverage are the high accuracy altimetry records that became available with the TOPEX-POSEIDON satellite beginning at the end of 1992, providing (at the time of writing) about 15 years of usable data. We now briefly describe the way in which altimetric data can be used to make some inferences about transport variability and the link between these inferences and the problem of trend determination. In practice, one seeks (Wunsch and Heimbach, 2009) to combine the altimetric data with *all* available oceanographic data, but the domination of the calculations by the volume of satellite data suggests the utility of the present focus.

*Corresponding author's e-mail: cwunsch@mit.edu

The major issue, and the one that provides the theme for the following discussion, is that altimetry produces estimates of the sea surface slope and hence of the surface geostrophic flow (to a high degree of approximation) and discussions of climate variables require inferences about the entire water column. Altimetry is only readily interpreted in volume (or mass) transport terms to the extent that the surface geostrophic flow is primarily controlled by, or controls, a known vertical structure. To interpret the results here, the approximation in Wunsch (1997) will be employed — that the *surface* kinetic energy is dominantly that of the first baroclinic mode. The expression 'transport' is then used as shorthand for the approximate volume transport in the first baroclinic mode above some arbitrary depth, possibly its zero crossing near 1000 m as used in Wunsch (2008). The reader is strongly cautioned, however, that as depicted in Wunsch (1997), and as discussed below, water column variability is dominated in many, if not most, places by the *barotropic* flow — which is sometimes arbitrarily omitted from theoretical discussions. Here the terminology 'barotropic' is used to denote the projection onto a vertically constant horizontal velocity as determined, for example, from a flat-bottom linear dynamics ocean. Lapeyre and Klein (2006) have shown that there can exist near-surface trapped balanced motions owing to a finite buoyancy flux through the sea surface. In the linear limit, these are the forced modes reviewed by Philander (1978). Motions not consistent with free modes can exist because they are externally forced, or because turbulent cascades generate them through non-linear interactions. But, at the present time, little observational data exist indicating their importance or vertical structure, and these surface-trapped motions are ignored in the following.

Let $\eta(x, y, t)$ be the surface elevation at any lateral point x, y, and let $\Delta\eta(y, t)$ be the difference $\eta(x + L, y, t) - \eta(x, y, t)$. If the vertical structure of a geostrophic flow field, $V(z)$, is known, then the total transport of volume or mass above any depth z_1, is readily computed as,

$$T(y,t) = \frac{g}{f}\frac{\Delta\eta(y,t)}{L} L\int_{z_1}^{\eta} V(z)dz = \frac{g}{f}\Delta\eta(y,t)\int_{z_1}^{\eta} V(z)\,dz \tag{1}$$

independent of L, as long as bottom topography does not intervene. We now explore the consequences of this relationship, for illustration purposes, in the region shown in Fig. 1 which occupies a large region of the subtropical gyre of the North Pacific Ocean. The western side is under the influence of the Kuroshio and its extension, while the eastern side may be regarded as typical of an oceanic interior. Pacific data are used here simply because they permit use of the largest distances and thus perhaps show the strongest spatial coherences.

Suppose now that the simplification is made that the water column structure $V(z) \propto F_1(z)$ where $F_1(z)$ is the first flat-bottomed baroclinic mode (Fig. 2), which has a zero crossing above about 1400 m (the shape is a slowly changing function of position). Consider the Archiving, Validation and Interpretation of Satellite Oceanographic (AVISO) gridded altimeter data (see Le Traon et al. (1998) for a discussion), at weekly intervals at the four corners of the box shown in Fig. 1. The time series for the altimetric heights are shown in Fig. 3; Fig. 4 displays their power densities. The latter have a general red noise character, becoming nearly white at periods longer than about three years. Records from the northern limit of the box show a weak annual cycle as indicated in the figure.

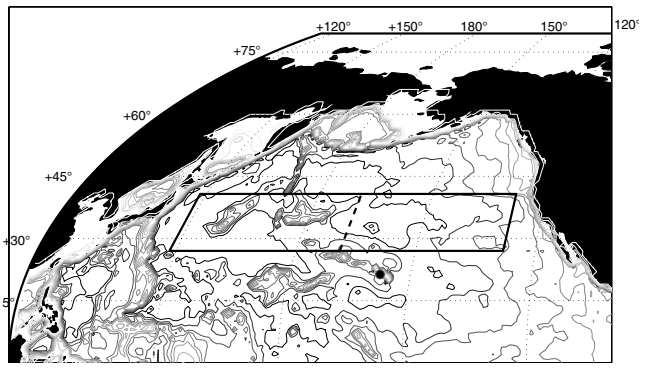

Fig. 1 Region used to study sea level and transport variability. Only the eastern half of the box (east of dashed line) is used for some of the spectral calculations to avoid the very energetic Kuroshio and Kuroshio extension region, but meridional transports are computed over the entire width.

Visually there is little resemblance among the time series. Of more immediate interest is the coherence related to the meridional volume transport. Figure 5 shows the coherence of $\Delta\eta$ over the box width at meridional separations of 1°, 3°, and 5° of latitude relative to the southern boundary of the box. With a latitudinal separation of 1°, there is high coherence, although not uniformly, down to periods as short as about 100 days. By 3° of latitudinal separation, there is no statistically significant coherence at 95% confidence until periods of almost three years are reached. At 5° of meridional separation, even 15 years of data produce no apparent coherence and what coherence there is would account for a very small fraction of the total variance.

These results are an extension to a much longer space scale of the results sketched by Wunsch (2008) who suggested that many decades would be required to obtain results indicative of circulation trends in the large-scale ocean circulation. (H. Johnson and D. Marshall, personal communication (2009) have suggested that eddy noise might be substantially reduced as one approaches the western boundary. Although that is possibly true for the North Atlantic near 25°N, the present results apply to the open ocean, and the increased energy toward the west, which is apparent in the power density spectra of Fig. 4, is consistent with expectations of the most elementary physics.)

The incoherence seen in Fig. 5 is not a consequence of the presence of the Kuroshio. Figure 6 shows the coherence

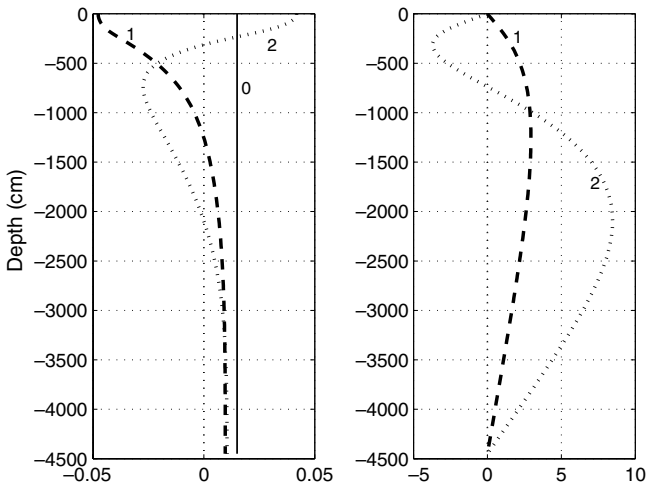

Fig. 2 Shapes of the first 3 modes (n = 0,...,2) at longitude λ = 220°E for horizontal velocity or pressure (left panel) and vertical displacement (right panel). Vertical displacements in the barotropic mode are linear with depth (increasing upwards) but much too small to be visible in the plot. Note that the surface boundary condition here precludes a buoyancy disturbance there — an issue of concern in a different context.

estimate for a 12° meridional separation using only the data east of the dashed line in Fig. 1. Thus, even in the reduced eddy energy region, there is no useful coherence at 12° latitudinal separation after 15 years. Whatever large-scale trends are present in the circulation are invisible here.

3 Frequency-wavenumber spectra

The lack of large-scale coherence and the general dominance of the spectra by low frequencies raises the question of the nature of the variability making up the altimetric records, and attention is now turned toward obtaining a partial understanding. One useful quantitative descriptor of oceanic variability is its frequency/wavenumber spectrum. Such a description, although incomplete because of the strong spatial inhomogeneity, is an essential element in determining the significance of apparent trends and other low frequency variations, and its reproduction is a central test of skill in a general circulation model. Zang and Wunsch (2001, hereinafter ZW2001) made an attempt to synthesize such a description from the data then available to them. A specific analogy to the original strawman internal wave model of Garrett and Munk (1972) was intended. The result assumed a restricted form of velocity component isotropy and did not represent the known anisotropic propagation of disturbances preferentially to the west. This supposedly universal form was spatially modulated by a complicated function of latitude and longitude independent of k,s. This paper discusses some of the elements needed in future attempts at an improved synthesis.

Since the ZW2001 work, the high accuracy altimetric record has been extended from the four years available to them to 15 years (at the time of writing), and this extended record opens the possibility of a more refined result. One element of the data — its representation of the altimetric data as showing 'too-fast' Rossby waves (Chelton and Schlax, 1996) — received a remarkable degree of theoretical attention, notwithstanding its subsequent repudiation by Chelton et al. (2007). The latter authors concluded that there is no evidence for linear Rossby waves (D. Chelton, private communication, 2009). Furthermore, the issue of the vertical structure, which was the focus of the mooring study of Wunsch (1997), has been put into context by theoretical and modelling studies (e.g., Smith and Vallis, 2001; Scott and Arbic, 2007; Ferrari and Wunsch, 2009) of the existence of both up- and downscale cascades in oceanic balanced motions. These discussions and debates have consequences for an improved representation of the frequency-wavenumber spectrum and ultimately its use in discussions of trend determination. Altimetric data now exceed in duration almost all oceanographic datasets and represent the only near-global dynamically relevant measurements that we have. Thus, their understanding is in turn central to the understanding of ocean circulation variability and the particular problem of trend determination. The present analysis is not comprehensive but is intended to call attention to some of the issues in understanding the mid-latitude variability producing the incoherent results of the previous section.

Visual displays of the altimetric behaviour in time and longitude (e.g., Fig. 7) show striking westward propagation of patterns and are usually interpreted as Rossby waves. Chelton and Schlax (1996) interpreted the visual phase lines as linear, first baroclinic mode Rossby waves and showed that their apparent phase velocity tended to be higher than predicted by theory.

It is worth listing the major assumptions underlying what it is reasonable to call the 'basic textbook theory' (BTT)[1] that was being compared to the observations. Those assumptions constitute a model of an ocean that

(1) has a flat bottom,
(2) has horizontally uniform stratification,
(3) is otherwise at rest,
(4) is represented by a tangent plane approximation to a sphere (the β–plane),
(5) is unforced,
(6) has completely linear dynamics, and
(7) is laterally unbounded.

This list is not complete (e.g., the Boussinesq approximation is also made). Of course, none of these assumptions is strictly correct and that the BTT works as well as it seems to is perhaps the real surprise.

Consider, as an example, the region shown in Fig. 1, the eastern side of the box used to discuss the transport variability. The region is a representative one (to the extent that any ocean region can be so described), at least of the subtropical gyres. The data are again the gridded fields provided by AVISO and smoothed using the algorithm of Le Traon et al.

[1]The long history of Rossby waves was summarized by Platzman (1968).

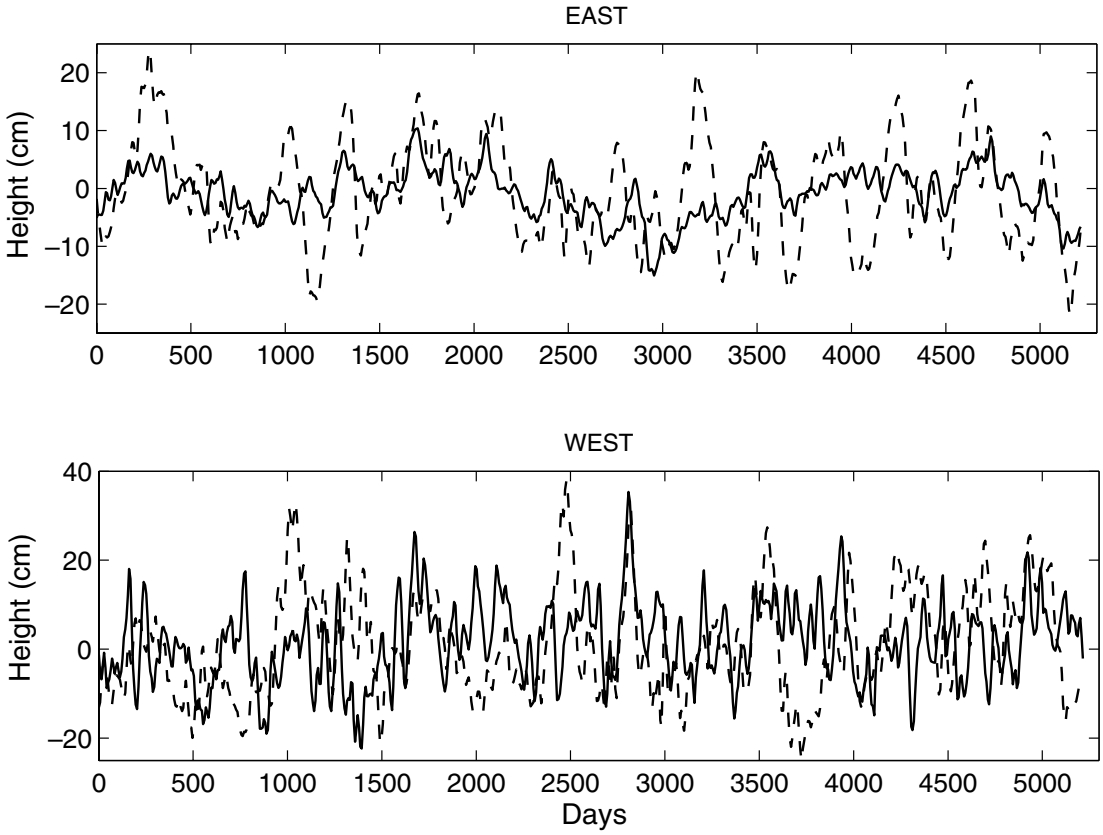

Fig. 3 The upper panel is the altimetric height at the southeast (solid) and northeast (dashed) corners of the box, and the lower panel shows the altimetric heights for the southwest (solid) and northwest (dashed) corners. It is apparent that there is little visual coherence.

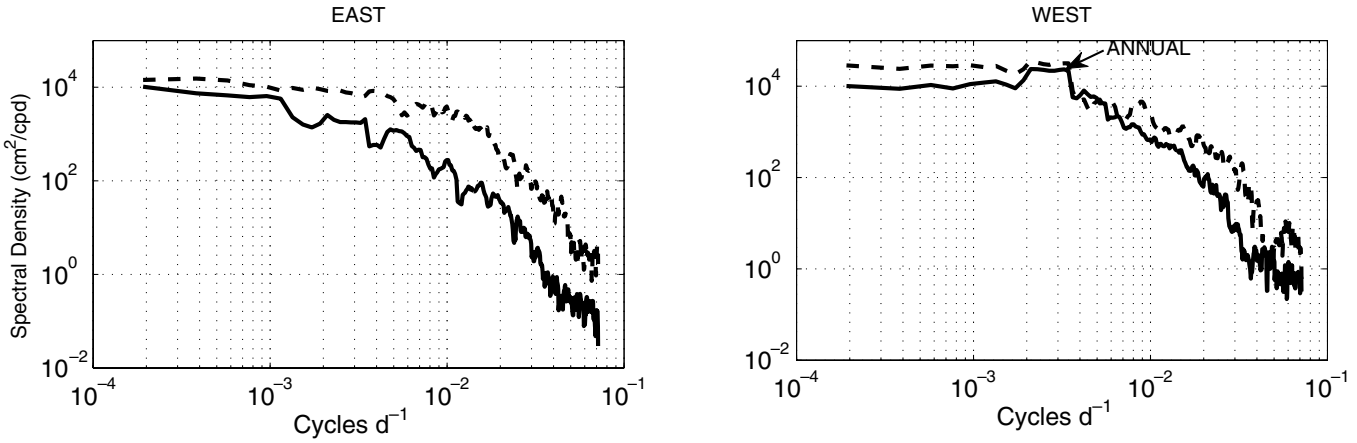

Fig. 4 Multi-taper spectral density estimates at the four corners of the analysis box. Because they are incoherent, the power density of the surface velocity between these two positions will be the sum of the spectra and thus dominated by that at the western end. Multi-taper spectral estimates are biased at the lowest frequencies and thus are slightly 'redder' than is apparent here.

(1998). Smoothing and gridding change the spectral content of a dataset, but in the present case it is not believed that this introduces any significant distortion. Figure 7 displays a time-longitude diagram for surface elevation, $\eta(x, y_c, t)$ along latitude 29.25°N in the box. The human eye is an extremely powerful instrument for pattern recognition and can very clearly detect the westward propagation in Fig. 7. The eye is not, however, very good at producing estimates of the other motions present — motions that produce less marked patterns. Zang and Wunsch (1999), using Fourier methods to separate different frequencies and wavenumbers, concluded that at the longest wavelengths and lowest frequencies, with about 40% of the observed variance, the motions had structures in frequency-wavenumber space indistinguishable from

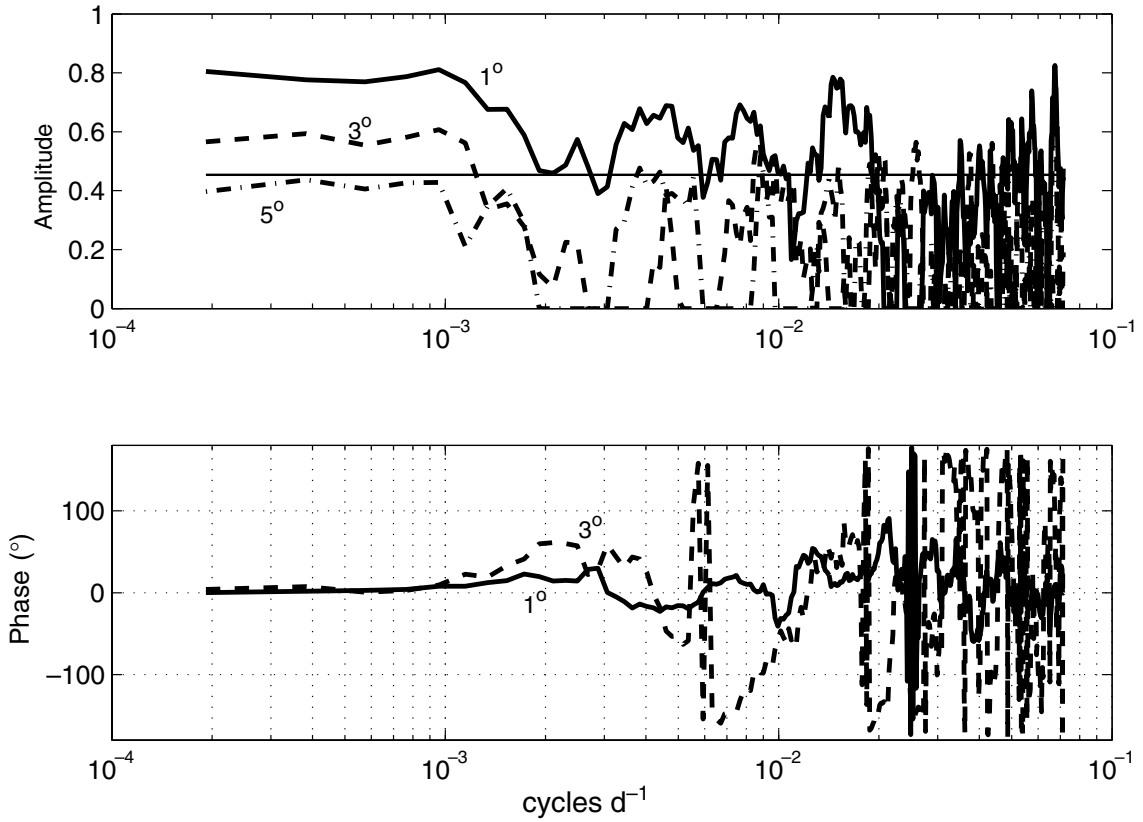

Fig. 5 A multi-taper coherence estimate of the apparent transport between the eastern and western sides of the box at meridonal separations of 1°, 3° and 5°. At 5° separation there is no apparent coherence even with 15 years of data and results for larger separations are not shown. An approximate level-of-no-significance at 95% confidence is indicated by the horizontal line. Phases are not statistically meaningful when the amplitude is below the level-of-no-significance and are thus not shown for separations beyond 3° latitude separation.

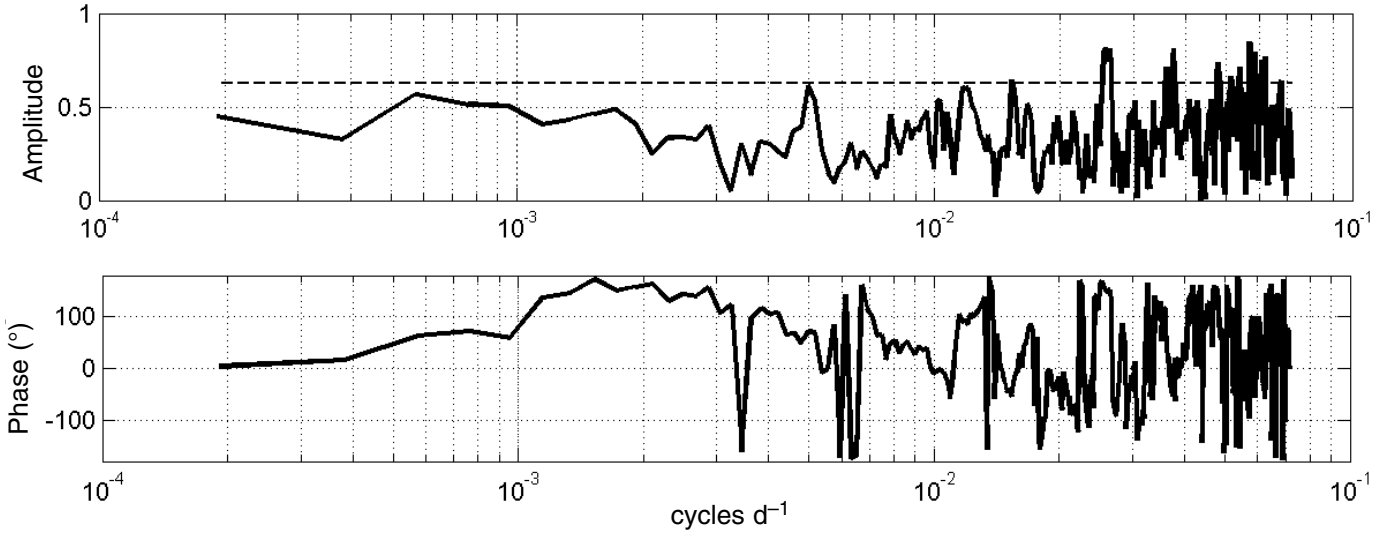

Fig. 6 As in Fig. 5 except over 12° meridional separation with the east-west separation taken from the centre of the box to the eastern boundary. There is no significant coherence at any frequency at this separation.

the BTT. As the wavenumber and frequency magnitudes increased, significant deviations from the BTT were plainly present — as Chelton and Schlax (1996) had pointed out. The results appeared to apply at all low and mid-latitudes of the North Pacific that they examined.

A full quantitative oceanic description, however, attempts to break the motions down by frequencies and wavenumbers, separates eastward/westward and northward/southward

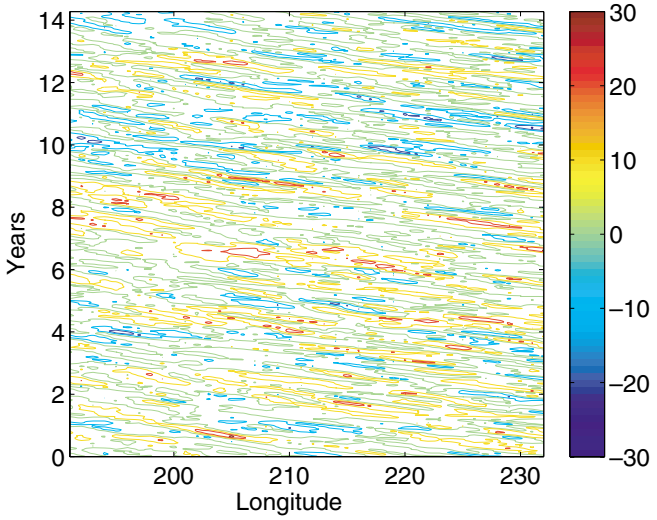

Fig. 7 Longitude/time diagram for sea surface elevation, η, (cm) at latitude 29.25°N in the area in Fig. 1, confined to the east of the obvious Kuroshio extension. The westward phase propagation is visually dominant and important but raises the question of how much of the variability is not described by these non-dispersive waves.

propagation, and distinguishes motions consistent with elementary theory from those requiring more complicated explanation. (Chelton and Schlax (1996) and several others (e.g., Lecointre et al. (2008) — a model study) have used a so-called Radon transform to determine the dominant phase velocity in these data. The Radon transform, perhaps best known in its tomographic applications (see Rowland, 1979), is computed by integrating the field along all straight pathways defined along all angles in data fields such as in Fig. 7. One can then find those path angles which maximize the integral and use them to define the signal phase velocity. All frequencies and wavenumbers contributing to the dominant phase velocity are grouped together. Of equal interest, however, is knowledge of the fraction of the total energy accounted for by that phase velocity band. Because the Radon transform can be converted into a Fourier transform (e.g., Rowland, 1979) its information content is neither more nor less than that of the Fourier approach used here. The information content of the Fourier transform is complete — as is the Radon transform if the integrals along *all* pathways are provided. Information by frequency and wavenumber band has typically proved enlightening in wave propagation problems, even those containing important non-linearities.)

Another consideration worth keeping in mind is that *phase velocity* structures in observed fields are commonly not fundamental physical properties of the motions. The best known discussion of the problem is probably that by Sommerfeld (1914) and Brillouin (1960) who showed that electromagnetic phase velocities exceeding the speed of light were not a contradiction to special relativity. Rather it was the group velocity, which has physical meaning as the rate and direction with which energy and information flow, that remained fundamental (see Brillouin (1960) for an extended discussion). In a general context, phase lines are kinematic interference patterns and so subject to distortion by a wide variety of phenomena including boundary positions. So for example, Frankignoul et al. (1997) point out that introducing an eastern wall in the presence of BTT Rossby waves immediately produces naively determined zonal phase velocities that are a factor of two larger than the BTT dispersion relationship, but see Lacasce (2000). A full Fourier procedure, as is used here, that accounts for standing wave components would not display such a discrepancy.

Figure 8 shows the estimated frequency-wavenumber spectra, $\Phi(k, s)$ for a fixed latitude (27° — the southern edge of the area) from a mildly smoothed periodogram (over two frequency and two wavenumber bands). The dispersion curves are shown for the barotropic and lowest vertical baroclinic mode with $l = 0$ and a first mode having a deformation radius, $R_d = 35$ km. Also shown are the cases when $k = 1$, producing unit aspect ratio linear waves. Consistent with the result of Zang and Wunsch (1999, their Figs 4 and 5), at the very lowest observable frequencies and wavenumbers, the energy maximum is indistinguishable from the dispersion curve. With increasing frequency (and corresponding wavenumber), deviations from the curve are seen, as pointed out by Chelton and Schlax (1996). Consistency with the dispersion curve of the BTT does not prove that those low frequency motions are BTT Rossby waves but does remove the main evidence that they are incompatible with it. For larger magnitude frequencies and wavenumbers, the deviation is quite marked, with higher apparent phase and group velocities and phase velocities tending toward the much higher values predicted for the barotropic mode. Finite l shifts the barotropic curve measurably closer to the baroclinic one.

The energy maximum lying approximately along the straight line $\gamma k + s = 0$, $\gamma \approx 4$ km d^{-1} is quite striking and as it implies non-dispersive motions, it will be called the 'non-dispersive line'. It reaches all the way from the lowest estimated frequency to the barotropic dispersion curve. As in Zang and Wunsch (1999), γ is approximately the long-wavelength (non-dispersive limit) group velocity of the first baroclinic mode. They found it to be universally present in all the areas they analyzed. No theory has so far explained this striking characteristic of oceanic variability. Note, however, that the peak at the annual cycle is indistinguishable from $k = 0$. Whether the non-dispersive line is truly tangent to the baroclinic dispersion curve as $s \to 0$ is not clear and as the period approaches infinity, many physical complications can ensue. From the results of Longuet-Higgins (1964), one might have anticipated an energy maximum where the zonal group velocity of the first baroclinic mode vanishes, where $\partial s/\partial k = 0$ (in analogy to the arguments of Wunsch and Gill (1976) for the equatorially trapped gravity modes), but there is no obvious evidence for such a structure here.

It is, of course, possible that a much stronger effective β, arising from the background potential vorticity gradient (e.g., Killworth et al., 1997), would push the non-dispersive, low wavenumber end of the first baroclinic mode dispersion curve to much higher values. That motions on the non-dispersive

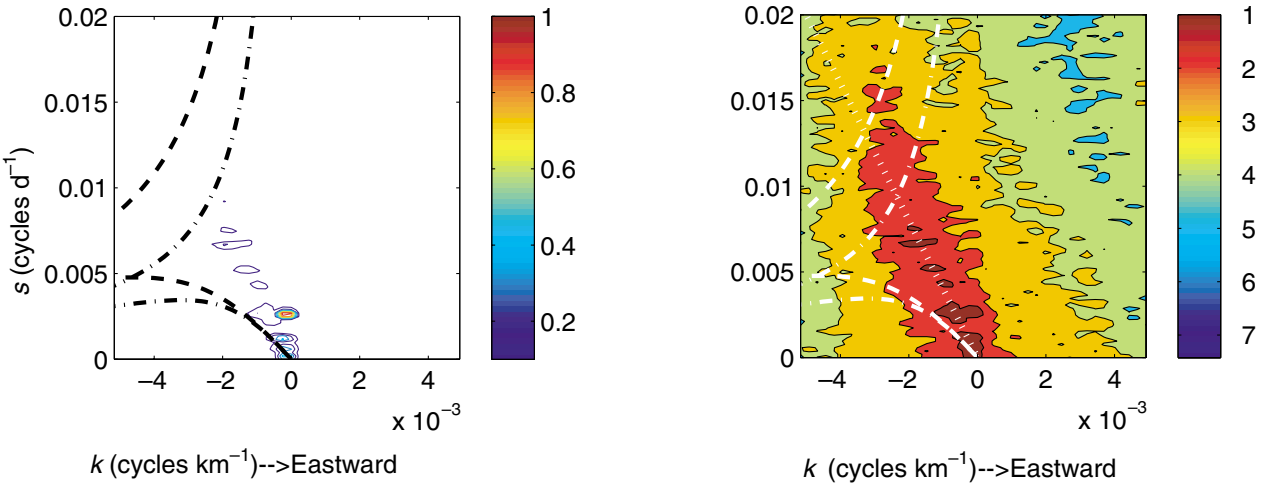

Fig. 8 Frequency (cycles d^{-1}) and zonal wavenumber (cycles km^{-1}) along the southern edge of the box. The left panel is from the two-dimensional periodogram plotted on a linear power scale, smoothed in frequency and wavenumber so as to be χ^2 variables with about eight degrees of freedom in each estimate (averaged over two frequencies and two wavenumbers). The right panel displays the logarithm of the power. Dashed curves indicate the barotropic and first baroclinic mode, $l = 0$, basic dispersion curves; dash-dot lines are the corresponding curves for the unit aspect ratio. The 'non-dispersive line' defined in the text lies along the ridge of maximum energy density and is closely approximated by the dotted white line (slope is 4 km d^{-1}).

line range from the baroclinic to barotropic mode dispersion curves suggests a coupling of these modes, with an implied vertical structure taken up in the following. Note that the zonal mean surface velocity over the entire area is about 0.05 cm s^{-1} and its rms value is about 0.2 cm s^{-1} and so is unlikely to cause first-order distortions in the dispersion relation. (It is important to recall, however, that the gridded altimetric data are smoothed, and thus will tend to underestimate the rms velocity field. Time means are also subject to errors in the estimated geoid.)

Some measure of the relative importance of the energy lying along the non-dispersive line is obtained by finding the cumulative sum over k, for each frequency, s, and normalizing it by the total

$$C(k,s) = \frac{\int_{-k_{\max}}^{k} \Phi(k,s)\,ds}{\int_{-k_{\max}}^{k_{\max}} \Phi(k,s)\,ds}$$

and which is plotted in Fig. 9 as a function of k for various values of s. At low frequencies, where the motions are indistinguishable from BTT Rossby waves, the non-dispersive line is the major fraction of the energy; at high frequencies, it has disappeared altogether as a noticeable feature. Thus, at periods shorter than about 100 days, the unstructured spectral model of ZW2001 is reasonably accurate, but it fails to account for the excess non-dispersive motions at low frequencies.

If the frequencies and wavenumbers are summed out, one obtains the zonal wavenumber, $\Phi_k(k)$ and frequency, $\Phi_s(s)$. That is,

$$\int_0^\infty \Phi(k,s)\,ds = \Phi_k(k), \tag{2}$$

$$\int_{-\infty}^{\infty} \Phi(k,s)\,dk = \Phi_s(s), \tag{3}$$

shown in Fig. 10. Φ_k shows the strong k^{-4} roll-off noted by Stammer (1997) on spatial scales shorter than about 500 km. (ZW2001 used $k^{-5/2}$ above 1/400 km.) In this particular region, the eastward-going variance is about 29% of the total, and its wavenumber spectrum has a different, near power-law, red-noise behaviour. Because Stammer (1997) used along-track data, the rapid roll-off is not a consequence of the mapping (smoothing) methodology employed at AVISO. The frequency spectrum here falls at a rate closer to s^{-3} than the s^{-2} value used by ZW2001 which, however, included the more energetic western part of the ocean. At low frequencies, a fit excluding the annual peak gives a power law close to $s^{-0.3}$, roughly consistent with ZW2001.

Figure 11 is a time-*latitude* diagram. Visually, the pattern is much more like a standing wave, although the amplitude modulation with latitude shows that wavenumbers other than $l = 0$ must be involved and they must be phase-locked. In the discussion of dispersion relations for the zonal motions, $l = 0$ was assumed for simplicity. Figure 12 shows the linear and logarithmic contours of (l, s) power density from the 15° latitude band across the box. While the energy is clearly clustered around $l = 0$, significant amounts are found at finite values. Figure 8 shows that there is finite energy at scales shorter than 1000 km but longer than the Rossby radii, that ultimately must be taken into account. In terms of the BTT dispersion relationship, finite l pushes all the baroclinic modes to yet lower frequencies, and thus has little effect on the structure near $s = 0$, where much of the energy is nearly tangent to the $n = 1$ curve. Note the slightly reddish nature of the low frequency spectrum.

4 Vertical structure

The discussion of transports as inferred from altimetry is directly dependent upon the vertical structure underlying the surface motions. In the schematic of Wunsch (2008), it was

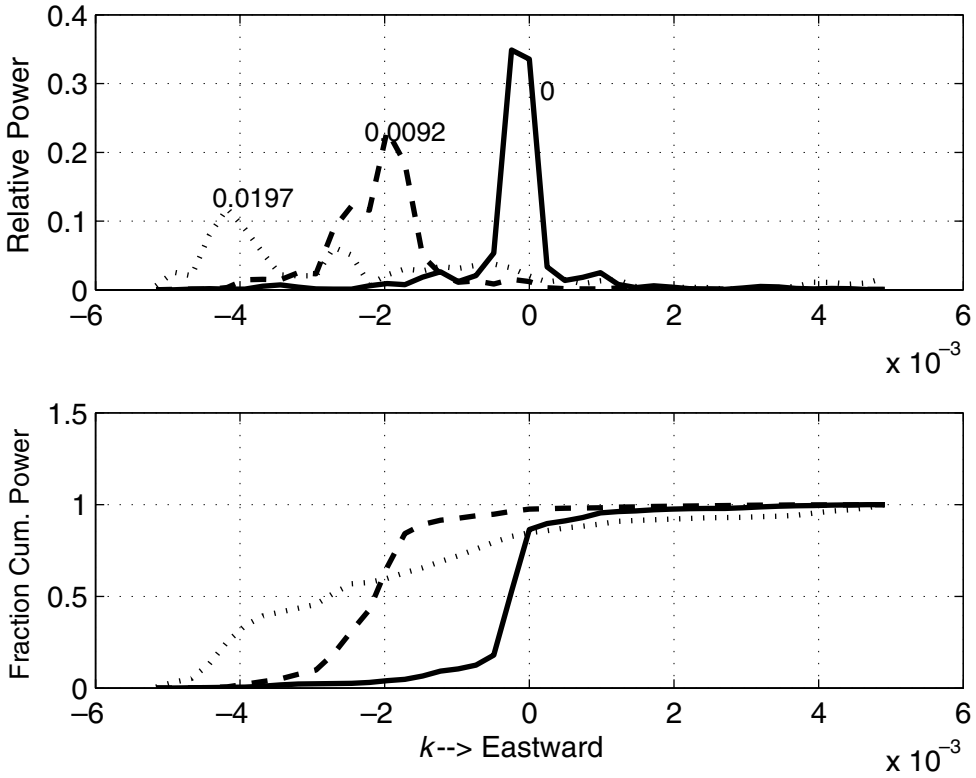

Fig. 9 The upper panel shows, three values of s in cycles d^{-1}, the values of the smoothed estimated power spectral density displayed in Fig. 8 and the lower panel shows the accumulating sum. Frequency separation is logarithmic between $s = 0$ and $s = 0.02$. The energy excess on the non-dispersive line is seen as a large near-jump in the integrated values. At the lowest frequencies, the neigbourhood of the non-dispersive line contains about 80% of the energy, falling to an undetectable excess about the background at the highest frequencies (the accumulating sum is nearly linear there). All values were normalized so that the sum of the power over k at fixed s is unity. Most of the low frequency energy is westward going, becoming more nearly equipartitioned at the highest frequencies.

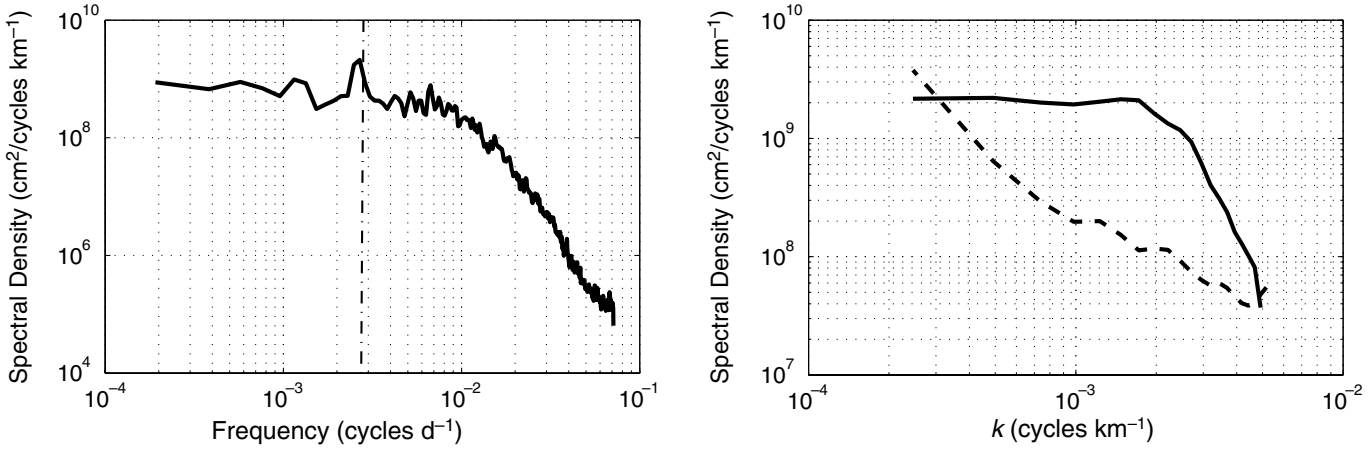

Fig. 10 Frequency, Φ_s (s) (left panel), and zonal wavenumber, Φ_k (k) (right panel) spectra of η for the eastern part of the study region. Wavenumber spectra are shown as westward- (solid) and eastward- going (dashed) energy. The vertical dashed-dotted line denotes the annual cycle which is only a small fraction of the total energy and which (see Fig. 8) is dominated by the lowest wavenumbers, indistinguishable here from $k = 0$. Approximate 95% confidence limits can be estimated as the degree of high frequency or wavenumber variability about a smooth curve and are quite small.

assumed that all of the motions lay in the first baroclinic mode. A rough rule of thumb is that about 50% of the mesoscale kinetic energy is in the barotropic mode (with 'barotropic' specifically defined in Section 2) with about 40% in the first baroclinic mode (Wunsch, 1997). This inference is based upon the current meter data available at that time and was used by ZW2001 as part of their spectral description. There was considerable evidence of 'phase-locking' of the modes in some regions, albeit the coverage was inadequate to generalize about it. Such phase-locking can be an indication

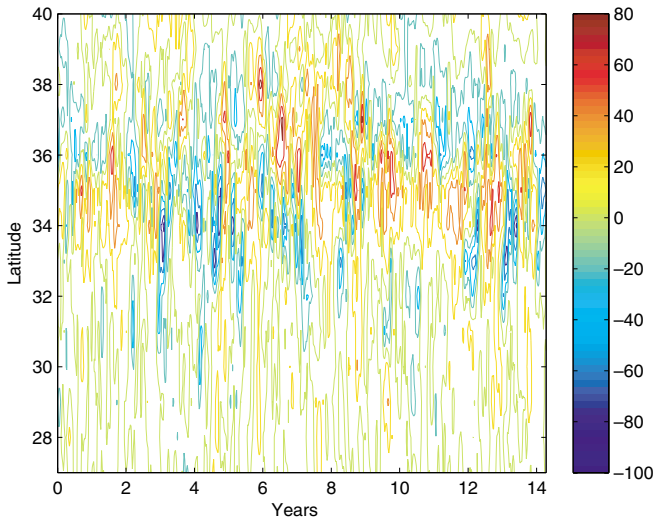

Fig. 11 A time-latitude diagram of sea surface height in centimetres along a meridional line (211°E) across the box in Fig. 1. Visually, the motions are close to standing oscillations in time and for simplicity are so regarded here, although the latitudinal wavenumbers are finite.

of non-linearity in the system, consistent for example with McWilliams and Flierl (1976) and the inference of Chelton et al. (2007) that a linear Rossby wave description is at best incomplete — as one infers from Fig. 2. Apparent phase-locking can also occur from the linear interaction of any particular vertical mode with topographic gradients — which necessarily then couple all the modes. Klein et al. (2008) discuss the plausible existence of trapped near-surface motions, dependent upon near-surface shear. Except for the existence of energy in frequency-wavenumber space in the altimetric records not coinciding with the BTT dispersion relations, there is no evidence that such motions are significant. In any event, vertical modes are a complete set, although possibly an inefficient one near $z = 0$ if surface buoyancy disturbances are important. If the modes are coupled, as they appear to be, a full description requires specification of their phase, in addition to their mean-square amplitude as a function of frequency.

With very rare exceptions, current meter records have a duration of less than one year and the set of water-column spanning current meter or temperature moorings of long duration is almost empty. The question then arises as to the vertical partition of oceanic kinetic energy on time scales exceeding that of geostrophic eddies (longer than about one year) and on spatial scales greater than a few hundred kilometres. A useful estimate is particularly important in the design of in situ arrays for trend determination in the general circulation. Using the global hydrography, Forget and Wunsch (2007) showed that vertical displacements could be interpreted in most regions as owing primarily, but not completely, to the first baroclinic mode. Hydrographic data used that way does not, however, permit any inferences about barotropic motions.

That the dominant observed motions are a combination of barotropic and baroclinic mode-like structures embedded in a broadband (in frequency and wavenumber) background of more linear motions is an inference consistent with the frequency-wavenumber content in Fig. 8, the 'too fast' phase velocity of Chelton and Schlax (1996), the coherent vortex picture of Chelton et al. (2007), and the coupled mode picture from current meter moorings of Wunsch (1997). The amount of information available about the details of the coherent vortex structures, which we tentatively identify with the non-dispersive line, is, however, minimal. We therefore propose, as a strawman hypothesis, that the energy density for the motions is proportional to the relative distances to the barotropic and first baroclinic mode dispersion curves with $l = 0$,

$$s = -\frac{\beta k}{k^2 + 1/R_i^2}, \quad i = 0, 1, \quad R_1 = 35 \text{ km}. \tag{4}$$

For numerical purposes, R_0 was set to infinity to avoid the presence of the longwave branch of the barotropic mode, which otherwise leads to a complicated multi-valuedness in the distance to the dispersion curve. Define r_0, r_1 as the minimum distance from any location, k^*, s^* to the two dispersion curves, Eq. (4), then their values are found numerically and plotted in Fig. 13.

A conjecture, based only on the fragmentary evidence already cited, is that we can partition the energy in the vertical as,

$$\frac{1}{r_1^2 + r_0^2}\left[r_1^2\left(1 - r_0^2\right)F_0^2(z) + r_0^2\left(1 - r_1^2\right)F_1^2(z)\right]$$

(not allowing for phase coupling), that is, depending upon the relative distances to the two dispersion curves. One could evidently extend such a rule to incorporate the distances to the dispersion curves of the higher baroclinic modes but, as we are essentially without any supporting information, that step is omitted here. Wunsch (1997) used the ratio of the surface kinetic energy computed directly from u, v to that computed from the sum of squares of the estimated modal amplitudes at the surface. Uncoupled modes should produce a ratio of one and wide variations, both above and below one were found, but no simple spatial pattern could be discerned. Most mooring records are too short to produce definitive results on modal coupling. Whatever the partition, it is important to note that many other structures are also present in the data.

5 Summary Comments

At the present time, the longest accessible periods are about 15 years, and the question of the nature of much lower frequency oceanic variability is open and requires separate study. Although eddy-resolving regional GCMs now exist, little or no data are available to test their conclusions. (The constrained state estimate with 1° horizontal resolution discussed by Wunsch and Heimbach (2008) shows a reduced,

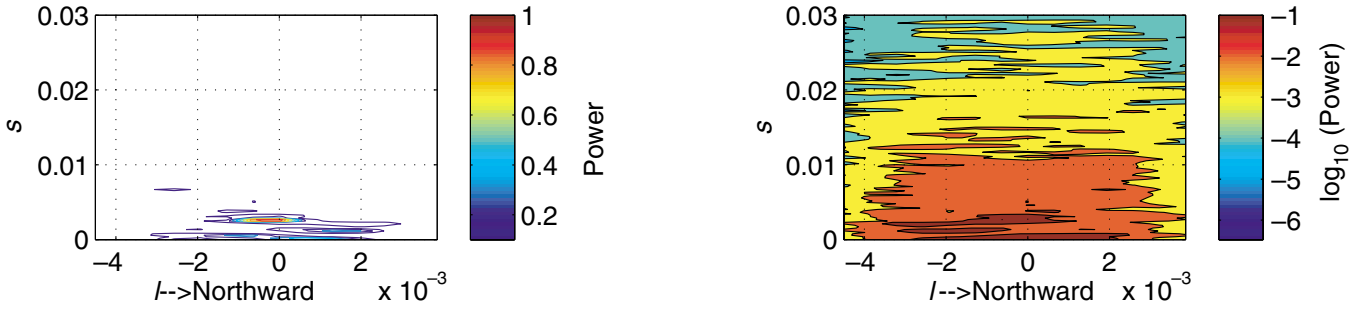

Fig. 12 Frequency-wavenumber (in l) spectra corresponding to Fig. 8. Somewhat more energy propagates northward than southward.

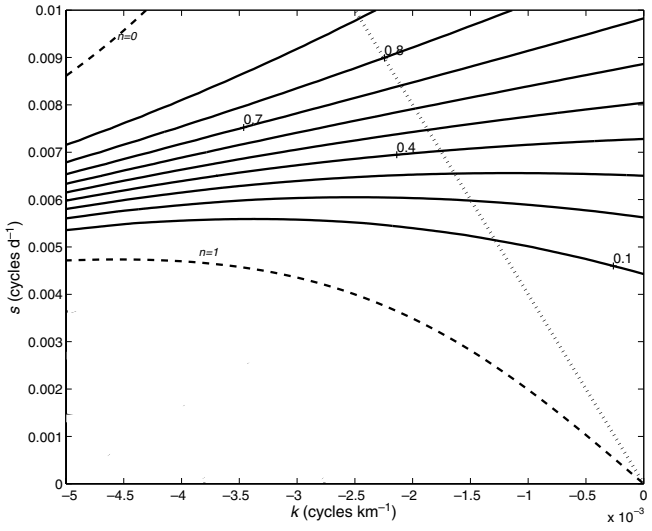

Fig. 13 Fraction of the variance hypothesized to lie in the barotropic mode and based upon the distance in k, s space from the two BTT dispersion curves (dashed lines), westward-going motions only. The dotted line is the non-dispersive line with an energy maximum and for which at low frequencies the motion would be almost completely baroclinic. At the present time, there is no information concerning the vertical structures for frequencies and wavenumbers lying below the $n = 1$ dispersion curve nor those above that for $n = 0$.

but non-zero, barotropic contribution at periods exceeding one year. No information is readily available to test that result and it is not discussed further.) To the extent that the altimetry of the particular subtropical region, supplemented by some mooring and other data, are typical of the global ocean, a few simple summary elements concerning the shorter periods, can be described.

Oceanic variability at these latitudes exhibits a broadband character in both frequency and wavenumber including significant eastward motions. Theory would suggest that much of this motion is forced meteorologically and/or is the result of turbulent cascades, but this inference has not been explored. At low frequencies and wavenumbers the motions are, from the proximity to the BTT dispersion curve, indistinguishable in altimetric data alone from linear Rossby waves.

In the band of frequencies from about 1 cycle per 15 years to about 1 cycle per 4 months, surface pressure variability (surface elevation) exhibits excess energy along the nearly non-dispersive line lying between the first baroclinic and barotropic modes. These motions are inferred to represent a non-linear coupling of these modes. It is *conjectured* that the relative fraction of the energy in the modes is inversely proportional to their distance in wavenumber-frequency space to the BTT dispersion curves and that the coherent eddies discussed by Chelton et al. (2007) are best described this way.

The origins of the non-dispersive motions have not been discussed. Coherent vortex dynamics, or Korteweg-DeVries types of soliton motions could be investigated, and some type of wave-turbulence interaction could conceivably give rise to such behaviour. It does seem to be a robust feature of the altimetric data.

Much more remains to be done, including making the analysis global (C. Hughes, personal communication, 2009) and in particular a special discussion of the Southern Ocean is needed — as it tends to be different in most ways. Better understanding of the meridional structure of the motions, theoretical understanding of the non-dispersive line and of the vertical partition of the energy are all needed. Alternative and perhaps more quantitatively accurate analytic frequency-wavenumber descriptions would be useful. How increasingly complex eddy-resolving general circulation models are to be tested is not obvious.

Acknowledgements

Useful comments were received from G. Flierl, R. Ferrari, P. O'Gorman, P. Cummins, D. Gilbert and two anonymous reviewers. This work was supported in part by the Jet Propulsion Laboratory (NASA) through the Jason-1 program, the National Ocean Partnership Program (NASA and NOAA). I thank Chris Garrett for providing the necessary excuse for a nice party and for many years of provocative interaction.

References

BRILLOUIN, L. 1960. *Wave Propagation and Group Velocity*. Academic, New York, 154 p.

CHELTON, D. and M. G. SCHLAX. 1996. Global observations of oceanic Rossby waves. *Science*, **272**: 234–238.

CHELTON, D. B.; M. G. SCHLAX, R. M. SAMELSON and R. A. DE SZOEKE. 2007. Global observations of large oceanic eddies. *Geophys. Res. Lett.* **34**(15): L15606, doi:10.1029/2007GL030812.

FERRARI, R. and C. WUNSCH. 2009. Ocean circulation kinetic energy: Reservoirs, sources, and sinks. *Ann. Rev. Fluid Mech.* **41**: 253–282.

FORGET, G. and C. WUNSCH. 2007. Estimated global hydrographic variability. *J. Phys. Oceanogr.* **37**: 1997–2008.

FRANKIGNOUL, C.; P. MÜLLER and E. ZORITA. 1997. A simple model of the decadal response of the ocean to stochastic wind forcing. *J. Phys. Oceanogr.* **27**: 1533–1546.

GARRETT, C. J. R. and W. H. MUNK. 1972. Space-time scales of internal waves. *Geophys. Astrophys. Fluid Dyn*. **3**: 225–264.

IPCC (Intergovernmental Panel on Climate Change). 2007. *Climate Change 2007 - The Physical Science Basis*. Cambridge Univ. Press, Cambridge, 1009 pp.

KILLWORTH, P. D.; D. B. CHELTON and R. A. DE SZOEKE. 1997. The speed of observed and theoretical long extratropical planetary waves *J. Phys. Oceanogr.* **27***:* 1946–1966.

KLEIN, P.; B. L. HUA, G. LAPEYRE, X. CAPET, S. LE GENTIL and H. SASAKI. 2008. Upper-ocean turbulence from high-resolution 3D simulations. *J. Phys. Oceanogr.* **38**: 1748–1763.

LACASCE, J. H. 2000. Baroclinic Rossby waves in a square basin. *J. Phys. Oceanogr.* **30**: 3161–3178.

LAPEYRE, G. and P. KLEIN. 2006. Dynamics of the upper oceanic layers in terms of surface quasigeostrophy theory. *J. Phys. Oceanogr.* **36**: 165–176.

LECOINTRE, A.; T. PENDUFF, P. CIPOLLINI, R. TAILLEUX and B. BARNIER. 2008. Depth dependence of westward-propagating North Atlantic features diagnosed from altimetry and a numerical 1/6 degrees model. *Ocean Sci.* **4**: 99–113.

LE TRAON, P. Y.; F. NADAL and N. DUCET. 1998. An improved mapping method of multisatellite altimeter data. *J. Atmos. Ocean. Technol*. **15**: 522–534.

LONGUET-HIGGINS, M. S. 1964. Planetary waves on a rotating sphere. *Proc. Roy. Soc. Lond. A*, **279**: 446–473.

MCWILLIAMS, J. C. and G. R. FLIERL. 1976. Optimal, quasi-geostrophic wave analysis of MODE array data. *Deep-Sea Res*. 23: 285–300.

PEACOCK, S. and M. MALTRUD. 2006. Transit-time distributions in a global ocean model. *J. Phys. Oceanogr.* **36**: 474–495.

PERCIVAL, D. B.; J. E. OVERLAND and H. O. MOFJELD. 2001. Interpretation of North Pacific variability as a short- and long-memory process. *J. Clim.* **14**: 4545–4559.

PHILANDER, S. G. H. 1978. Forced oceanic waves. *Rev. Geophys.* **16**: 15–46.

PLATZMAN, G. 1968. The Rossby wave. *Q. J. R. Meteorol. Soc*. **94**: 225–248.

ROWLAND, S. W. 1979. Computer implementation of image reconstruction formulas. In: *Image Reconstruction from Projections. Implementation and Applications*. G. T. Herman (Ed.) Springer-Verlag, Berlin, pp. 9–80.

SCHIERMEIER, Q. 2004. Gulf Stream probed for early warnings of system failure. *Nature*, **427**: 769.

SCOTT, R. B. and B. K. ARBIC. 2007. Spectral energy fluxes in geostrophic turbulence: Implications for ocean energetics. *J. Phys. Oceanogr.* **37**: 673–688.

SMITH, K. S. and G. K. VALLIS. 2001. The scales and equilibration of midocean eddies: Freely evolving flow. *J. Phys. Oceanogr.* **31**: 554–571.

SOMMERFELD, A. 1914. Über die Fortpflanzung des Lichtes in dispergierenden Medien. *Ann. d. Phys.* **44**: 177–202.

STAMMER, D. 1997. Global characteristics of ocean variability estimated from regional TOPEX/POSEIDON altimeter measurements. *J. Phys. Oceanogr.* **27**: 1743–1769.

WUNSCH, C. 1997. The vertical partition of oceanic horizontal kinetic energy. *J. Phys. Oceanogr.* **27**: 1770–1794.

WUNSCH, C. 2008. Mass and volume transport variability in an eddy-filled ocean. *Nature Geosci.* **1**: 165–168.

WUNSCH, C. and A. E. GILL. 1976. Observations of equatorially trapped waves in Pacific sea level variations. *Deep-Sea Res.* **23**: 371–390.

WUNSCH, C.; R. PONTE and P. HEIMBACH. 2007. Decadal trends in global sealevel patterns. *J. Clim.* **20**: 5889–5911.

WUNSCH, C. and P. HEIMBACH. 2008. How long to oceanic tracer and proxy equilibrium? *Quat. Sci. Rev.* **27***:* 637–651.

WUNSCH, C. and P. HEIMBACH. 2009. The global zonally integrated ocean circulation (MOC), 1992–2006: Seasonal and decadal variability, *J. Phys Oceanogr.* **39**: 351–368.

ZANG, X. and C. WUNSCH. 1999. The observed dispersion relation for North Pacific Rossby wave motions, *J. Phys. Oceanogr.* **29**: 2183–2190.

ZANG, X. and C. WUNSCH. 2001. Spectral description of low frequency oceanic variability. *J. Phys. Oceanogr.* **31**: 3073–3095.